ADAPTATION OF AN ECOLOGICAL TERRITORIAL MODEL TO STREET GANG SPATIAL PATTERNS IN LOS ANGELES

LAURA M. SMITH AND ANDREA L. BERTOZZI

University of California Los Angeles
Department of Mathematics
520 Portola Plaza
Box 951555
Los Angeles, CA 90095-1555, USA

P. JEFFREY BRANTINGHAM

University of California Los Angeles
Department of Anthropology
375 Portola Plaza
341 Haines Hall, Box 951553
Los Angeles, CA 90095-1553, USA

GEORGE E. TITA AND MATTHEW VALASIK

University of California Irvine
Department of Criminology, Law and Society
2340 Social Ecology II
Irvine, CA 92697-7080, USA

ABSTRACT. Territorial behavior is often found in nature. Coyotes and wolves organize themselves around a den site and mark their territory to distinguish their claimed region. Moorcroft et al. model the formation of territories and spatial distributions of coyote packs and their markings in [33]. We modify this ecological approach to simulate spatial gang dynamics in the Hollenbeck policing division of eastern Los Angeles. We incorporate important geographical features from the region that would inhibit movement, such as rivers and freeways. From the gang and marking densities created by this method, we create a rivalry network from overlapping territories and compare the graph to both the observed network and those constructed through other methods. Data on the locations of where gang members have been observed is then used to analyze the densities created by the model.

1. **Introduction.** Street gangs have a long history in Los Angeles [35, 46] and are major contributors to violent acts in the region [17, 34, 36, 47, 38]. Gangs compete to secure both instrumental (e.g., money, drugs, space) and expressive (e.g., reputation, power) resources, often causing a partitioning of the city into gang territories [43]. Disputes over spatial resources may lead to violence and acts of retribution, augmenting or creating a rivalry between gangs [11, 44]. One common method for a gang to mark its territory is through the use of graffiti [2, 10, 30]. Our goal is to model the spatial behaviors for gangs and their taggings.

One approach for modeling human behavior is through the framework of ecological models. The ecological models for optimal foraging have been applied to hunters and gatherers [20] and to people seeking information [40]. College drinking patterns have also been modeled through an ecological approach [1]. Ecology has been essential to epidemiological modeling of wildlife populations and diseases [26]. These models have in turn been applied to humans for not only infectious diseases, but also to the social sciences through the spread of ideas [7] and political affiliations [39]. Several models have recently been proposed to describe the territorial behavior of species as diverse as wolves [6, 9, 28, 29, 50], coyotes [32, 33], killer wasps [12], chimpanzees [49], foxes [18], and birds [25]. Some species, such as wolves, claim spatial regions via scent marking or other means [37]. Using gang graffiti as a proxy for scent marking, we can apply these ecological models to street gangs.

This paper examines the formation of gang territories and territorial markings by adapting the approach given in [33] that is based on a system of partial differential equations. Section 2 describes this approach for coyotes and the modifications made to model street gangs. Section 3 provides information on Hollenbeck, the eastern most policing division in the city of Los Angeles, which is the site of the case study where this model is applied. The implementation details are given in Section 4, and a description of the data sets are provided in Section 5. The results follow in Section 6. Section 7 concludes the paper with a discussion of the model implications.

2. **Modeling street gangs.** This paper develops a model to describe the equilibrium densities of gangs and gang graffiti. Gang graffiti marks the boundaries of contested regions claimed by multiple gangs, which may make these areas more prone to violence. Gang territories are dynamic and the boundaries change over time with the emergence of new gangs and other gangs collapse. The creation of a flexible model incorporating these fluctuations allows for the testing of theories while investigating system dynamics given certain changes [13, 19].

2.1. **Existing gang models.** Several models have recently been proposed for analyzing various gang behaviors. Retaliatory behavior among gangs has been simulated via self-exciting point processes [14, 41]. These methods focus on the temporal aspect of gang violence. Using this gang characteristic of retaliation, attempts have been made to fill in the missing data of which gang is responsible for a crime [21, 42]. From a different perspective, the authors of [4] use an approach from epidemiology to simulate membership in gangs.

A recent bottom-up approach examines the formation of rivalries. In [22], the authors propose an agent-based model that is coupled to a rivalry network. A node of the network represents a geographic position that is the central location to a gang's activities known as a set space [38, 45]. An edge in the network is present if there is a rivalry between the two gangs. In this stochastic model, agents move about the city and interact with members of other gangs. Once two gang members of different gangs cross paths, the weight of the edge between their two respective nodes is increased. This edge weight directly impacts the directional decisions the agents make, which is biased towards their home set space and away from rival gangs' set spaces and selected from a von Mises distribution [24]. Additionally, geographic boundaries in the region are incorporated into this model to restrict movement across rivers and large freeways. The model we propose here will include these geographic boundaries and compare the resulting rivalry network with those obtained in [22].

The Lotka-Volterra competition model has been used to analyze the creation of territorial boundaries between two gangs in [8]. Through this approach, the authors examined the locations of violent interactions with respect to the theoretical boundary between the two gangs and concluded that violence typically clusters about this dividing curve. Another model uses graffiti as the mechanism for interactions between gang members and analyzes the circumstances under which territories are formed [5]. Both of these methods focus only on situations with two gangs. In order to fully examine a system of twenty-nine active gangs in Hollenbeck, we will consider another approach taken from ecology.

2.2. **Ecological territorial models.** Many species exhibit territorial behavior, where individuals and/or groups are willing to defend space they currently hold from incursions by members of the same species (intraspecific competition) or other species (interspecific competition). These territorial behaviors are also exemplified by street gangs which use violence to control local drug markets or simply defend their neighborhood from outsiders. We consider existing ecological territorial methods to model these gang territorial behaviors. The paper [23] provides a review of partial differential equation models proposed for studying the spatial distributions of species. Some approaches include diffusion models, diffusion with drift and convection models, biased random motion models, models with aggregation or repulsion that depends on the current organism density, and models that depend on environmental features. Additionally, reaction-diffusion and predator-prey models incorporate competition into the system.

Two competing groups might never physically meet, yet still have defined territories. Coyotes and wolves are animals that exhibit territorial behavior through raised leg urination. When an individual comes in contact with a marking from a different pack, the animal increases its own urination and may move towards its home den located on the interior of its territory [28]. This avoidance of markings has been incorporated into wolf [6, 9, 28, 29, 50] and coyote models [32, 33] through a coupled system of partial differential equations for both the pack densities and the marking densities. These mechanistic home range models have recently been connected to models of resource selection analysis (RSA) [31]. One of the models of [33] includes a mechanism to avoid areas where the terrain is steep, and it is this model that we will modify to examine the spatial behaviors of street gangs.

2.3. **The proposed gang behavioral model.** Traditional gangs and territorial animals have distinctly claimed areas that are well-established [27]. They use markings to inform members of both their own group as well as other groups of territorial boundaries. Individuals may respond to markings of other groups by increasing their own marking density and by biasing their movement towards their respective den site for animals or set space for gangs. A gang's *set space* is the central location to the gang's activities [38, 45]. These behavioral characteristics and geographical considerations are incorporated into the "steep terrain avoidance plus conspecific avoidance (STA+CA)" model of [33] for coyotes. This model solves the following non-dimensionalized system to steady-state:

$$\frac{du^{(i)}}{dt} = \Delta u^{(i)} - \nabla \cdot \left[\beta \mathbf{x}_i u^{(i)} \sum_{j \neq i}^{n} p^{(j)} \right] + \nabla \cdot \left[\alpha u^{(i)} \nabla z \right] \tag{1}$$

$$\frac{dp^{(i)}}{dt} = u^{(i)} \left[1 + m \sum_{j \neq i}^{n} p^{(j)} \right] - p^{(i)}, \tag{2}$$

where for a given pack i, $u^{(i)}(x, y)$ is the expected population density, $p^{(i)}(x, y)$ is the expected marking density, and $\mathbf{x}_i$ is the unit vector to the home den site from the current location. The parameters β, m, and α represent the strengths to avoid markings, to increase one's own markings, and to avoid steep terrain, respectively. This system also has the boundary conditions on $\partial \Omega$

$$0 = \left[\nabla u^{(i)} - \beta \mathbf{x}_i u^{(i)} \sum_{j \neq i}^{n} p^{(j)} + \alpha u^{(i)} \nabla z \right] \cdot \overrightarrow{\mathbf{n}}, \tag{3}$$

where $\overrightarrow{\mathbf{n}}$ is the outward unit normal vector.

The system in Equations (1) and (2) models population densities and marking densities for a set of coyote packs. We now modify the approach for street gangs by letting $u^{(i)}(x, y)$ be the expected gang density, $p^{(i)}(x, y)$ be the expected graffiti density, and $\mathbf{x}_i$ be the unit vector to the set space of gang i from the current location. In this system, the term $\Delta u^{(i)}$ describes random motion of individuals. Since gangs typically avoid the territories of other gangs [3, 30] unless they are conducting a violent raid, they are more likely to return towards their set space when confronted by another gang's tags. This behavior is represented by the term $-\nabla \cdot \left[\beta \mathbf{x}_i u^{(i)} \sum_{j \neq i}^{n} p^{(j)} \right]$, where individuals that come in contact with any markings that are not of their own gang move in the direction towards home, $\mathbf{x}_i$. Equation (2) describes the process by which individuals increase their production of markings after discovering another gang's markings.

The $z(x, y)$ in the model is the elevation of the terrain for coyotes, but we use this term to incorporate other spatial features. We first determine geographical landmarks that could inhibit movement across them, such as rivers, freeways, and major roads. These features are not impassible, but there are limited bridges and underpasses available. Let $\Omega \subset \mathbb{R}^2$ be the set of points where there is a landmark. Consider the minimum Euclidean distance to the set Ω,

$$d(x, y) = \min_{(x_0, y_0) \in \Omega} \left\{ \sqrt{(x - x_0)^2 + (y - y_0)^2} \right\}.$$

We then define $z(x, y)$ to be

$$z(x, y) = 1 - \tanh \left(d(x, y)^2 \right).$$

This gives a "steep terrain" that gang members will avoid. Geography is therefore incorporated into the movement dynamics through the final term in Equation (1), $\nabla \cdot \left[\alpha u^{(i)} \nabla z \right]$, where each landmark is treated equally.

This partial differential equation approach has many features similar to the agent-based model proposed in [22]. Both models incorporate the geography as semi-permeable boundaries. Additionally, individuals engage in random movement, but have a bias towards their home set space. In the supplementary material for [33], the authors derive the model given in Equations (1) and (2) by using a von Mises distribution for the advection term. Thus, both models utilize the von Mises distribution to generate directionally biased motion. One major difference between the two methods is that the agent-based approach is stochastic, whereas the proposed model is deterministic with a derivation based on a stochastic process. Due

to the similarities in these models, we will also use Hollenbeck as the case study and compare the results to those given in [22].

3. **Street gangs in Hollenbeck.** The city of Los Angeles is plagued by gang violence. Hollenbeck, the eastern most division of the Los Angeles Police Department, is home to twenty-nine active Latino street gangs in only 15.2 square miles [38, 46]. Due to the geography of the area, the rivalries among the gangs in this region are generally restricted to Hollenbeck. Most of the rivalries and disputes among these gangs is linked to neighborhood-based territoriality rather than drugs or other conflicts.

To examine the structure of the rivalries in Hollenbeck, we view a graph that is embedded in space with nodes representing the set spaces of the gangs. If a rivalry exists between two gangs, then an edge is present between the two respective nodes. Among the twenty-nine gangs in Hollenbeck, there are sixty-nine observed rivalries. This observed network has been examined in [22, 38, 46]. The authors of these papers argue that the structure of this network is highly dependent on the geography of the region and the highways and rivers that pass through the area. Five major freeways, I-5, I-10, I-710, CA-60, and US-101, divide Hollenbeck into many sections. Figure 1 shows the spatially embedded rivalry network and the features that partition the region. It is clear that these physical boundaries impact the rivalry structure by limiting the number of rivalries between gangs in separate sections.
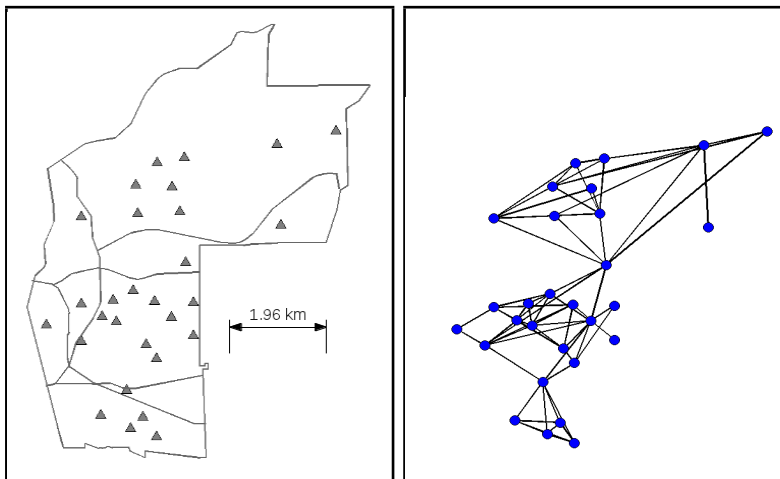

FIGURE 1. Set spaces embedded in Hollenbeck (Left) and the corresponding observed rivalry network (Right). Each solid triangle on the left and solid circle on the right gives the location of a gang's set space. The faint curves (Left) show the major roads and rivers that pass through the region, impacting the rivalry structure. The policing division boundary is also included as the bottom and right boundaries. The observed network from [38] is displayed on the right, where an edge between two gangs indicates an existing rivalry between the gangs.

4. **Implementation details.** For the G gangs, the model consists of a coupled system with $2G$ differential equations. We implemented this system by using finite differences and solving until steady-state. For each time step Δt, we loop through all of the gangs, updating first the $u^{(k)}$ and then $p^{(k)}$. For initialization, $u^{(k)}$ is set to be zero everywhere except at the location of the kth set space, where it has the value one. Alternatively, $p^{(k)}$ is initialized to be $\frac{1}{NM}$ everywhere, where the grid is $N \times M$. The discretized equation for the interior of $u^{(k)}$ at time $n + 1$ is given by

$$
\begin{aligned}
\frac{u_{i,j}^{(k),n+1} - u_{i,j}^{(k),n}}{\Delta t} &= \frac{1}{(\Delta x)^2} \left(u_{i+1,j}^{(k),n} - 2u_{i,j}^{(k),n} + u_{i-1,j}^{(k),n} \right) \\
&+ \frac{1}{(\Delta y)^2} \left(u_{i,j+1}^{(k),n} - 2u_{i,j}^{(k),n} + u_{i,j-1}^{(k),n} \right) \\
&- \frac{\beta}{2\Delta x} \left(u_{i+1,j}^{(k),n} \, x_{i+1,j}^{(k)} \sum_{l \neq k} p_{i+1,j}^{(l),n} - u_{i-1,j}^{(k),n} \, x_{i-1,j}^{(k)} \sum_{l \neq k} p_{i-1,j}^{(l),n} \right) \\
&- \frac{\beta}{2\Delta y} \left(u_{i,j+1}^{(k),n} \, y_{i,j+1}^{(k)} \sum_{l \neq k} p_{i,j+1}^{(l),n} - u_{i,j-1}^{(k),n} \, y_{i,j-1}^{(k)} \sum_{l \neq k} p_{i,j-1}^{(l),n} \right) \\
&+ \frac{\alpha}{\Delta x} \left(u_{i+1,j}^{(k),n} \, \nabla_x \, z_{i+1,j} - u_{i,j}^{(k),n} \, \nabla_x \, z_{i,j} \right) \\
&+ \frac{\alpha}{\Delta y} \left(u_{i,j+1}^{(k),n} \, \nabla_y \, z_{i,j+1} - u_{i,j}^{(k),n} \, \nabla_y \, z_{i,j} \right).
\end{aligned}
$$

The boundary of $u^{(k)}$ is updated using first order Neumann boundary conditions. Given this update of $u^{(k)}$, we then update both the interior and boundary of $p^{(k)}$ as

$$
\frac{p_{i,j}^{(k),n+1} - p_{i,j}^{(k),n}}{\Delta t} = u_{i,j}^{(k),n+1} \left(1 + m \sum_{l \neq k} p_{i,j}^{(l),n} \right) - p_{i,j}^{(k),n+1}. \tag{4}
$$

After this update, we ensure that $p^{(k)}$ is still a density that sums to one. After obtaining our final estimates for the gang and marking densities, we determine that a rivalry exists between two gangs if the regions where densities are non-negligible sufficiently overlap.

5. **The data sets.** In order to test the algorithm, we will use two different data sets. The first covers the years 1999 to 2002 and gives the locations of violence between two gangs. We only use the 340 events where both the suspect and victim gang are known and both are also in the set of twenty-nine Hollenbeck gangs. In [8], the authors compared the locations of events relative to the theoretical midline boundary between gangs. They concluded that violent interactions frequently cluster about this line. From this analysis, we should expect a higher density of violent events near the boundaries of territories where there is an increase in graffiti. For our model, this is where the markings, $p^{(i)}$, have a high density. Thus, we will compare our marking densities to this set of *violence data*.

The second set of data we have to evaluate our model gives the locations of where known or suspected gang members were stopped by the police. In such encounters, the officer fills out a Field Interview (FI) card, listing information about where the interaction took place and all individuals involved. These encounters are not initiated by violent events, and so we assume that these data are a sample of the

gang densities, $u^{(i)}$. This data set of 1,079 events, covering the year of 2009, will be referred to as *FI data*. Both data sets can be seen in Figure 2. Due to the large number of gangs, only the aggregated data will be displayed here.
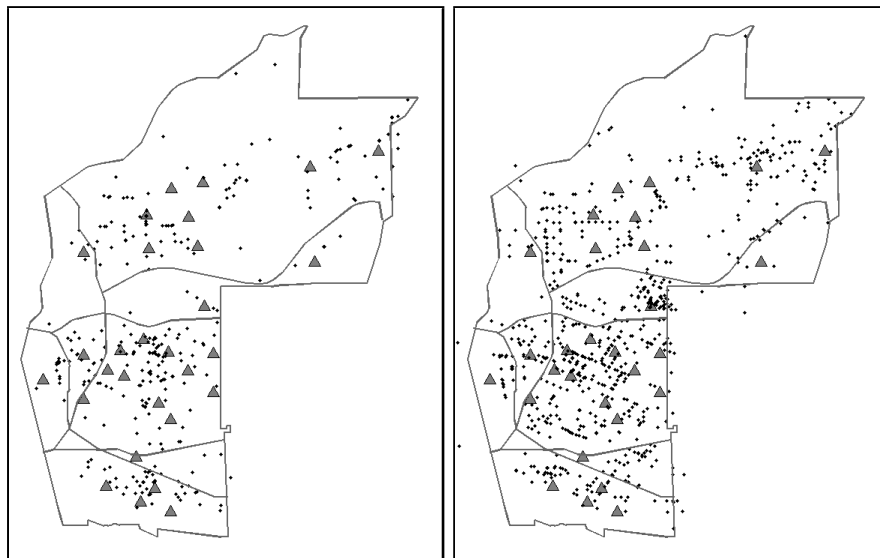

FIGURE 2. Violence and Field Interview data in Hollenbeck. The set spaces are given by solid triangles in both images. The gang violence data (Left) and Field Interview data (Right) are given by solid circles.

There is a possibility of errors in any data set, including inaccuracies, incompleteness, under-reporting of events, and bias [13]. Furthermore, for the data sets we are using, we should be cautious in the expectation that $p^{(i)}$ fully approximates the violence data and $u^{(i)}$ fully approximates the FI data. The nature of the sampling frame for the FI data is not perfectly understood, and there may be significant under-reporting of all but the most serious violent crimes. It should be noted that while not every encounter may produce an FI, law enforcement needs to continually document gang members activity with their gang and fellow affiliates for prosecution in future crimes. Regularly documenting activity, especially individuals loitering together, showcases this gang acuity to criminal justice actors. Additionally, it is reasonable to assume that a large number of these events can be predicted by the densities obtained by the model.

Another potential issue to consider is the difference in time frames for each set of data. The locations of the set spaces were taken from [38] published in 2010. Some set spaces may have moved during the eight years after the violence data was collected. As cities are ever changing, gangs may have adapted to the altered environments. For example, one housing area was redeveloped, forcing several Cuatro Flats, TMC, and Primera Flats gang members to relocate. This caused these gangs to ultimately have new set spaces. For simplicity, we will only use the original set space in our model implementation.

6. **Results.** With this implementation of the model for the Hollenbeck gangs, we optimize the parameters with respect to the accuracy metric for the rivalry network, defined in Equation (5) of Section 6.1. Additionally, we must ensure that the parameter m is large enough to produce a marking density that is not nearly identical to the gang density. Listed in Table 1 are the parameters used for this analysis.

Parameter	Value
m	100
β	1
α	1
Δt	0.001

TABLE 1. Parameter choices for the ecological territorial model.

We first compare our simulated network with that of the agent-based approach of [22] in Section 6.1. From here, we investigate the resulting gang and marking densities in Section 6.2. Given these densities, Section 6.3 estimates gang territory locations. One standard method for partitioning a region is through Voronoi diagrams, which we further discuss in Section 6.4. We then use the estimated territories to investigate the relationship with the two data sets in Section 6.5. Finally, we examine pairs of rival gangs and the locations of events with respect to the theoretical territories in Sections 6.6 and 6.7.

6.1. **Rivalry networks.** To create a rivalry network from the ecological territorial model, we must determine what quantifies a rivalry. If the violence among gangs in Hollenbeck is primarily attributed to territorial issues, then we would expect a rivalry to exist if the densities of two gangs sufficiently overlap. We thus threshold the densities to produce an approximate territory, and then find the overlapping area between pairs of territories. Since there are 69 empirically known rivalries among the gangs in Hollenbeck, we select the top 69 area pairs to construct a network. The resulting rivalry network obtained from the simulation is given in Figure 3, together with the observed network and the Simulated Biased Lèvy walk Network (SBLN) obtained in [22].

We notice that the ecological territorial model correctly identifies 45 of the 69 edges in the observed network. Additionally, this simulated network has similar graph properties with both of the other networks. To better quantify this similarity, we examine a few graph metrics that were previously used in [22].

We would like to inspect the accuracy of the simulated network. Initially, we calculate the number of true positives (TP), true negatives (TN), false positives (FP), and false negatives (FN). An edge is considered a true positive when it is correctly identified as an existing edge in the model and is present in the observed network, and it is a true negative when it is correctly identified as not being an edge. Alternatively, an edge is marked as a false positive if the simulation identifies it as an edge when it is not present in the observed network, and it is a false negative if the simulation fails to label a true rivalry as an edge. From these we calculate the *accuracy* score

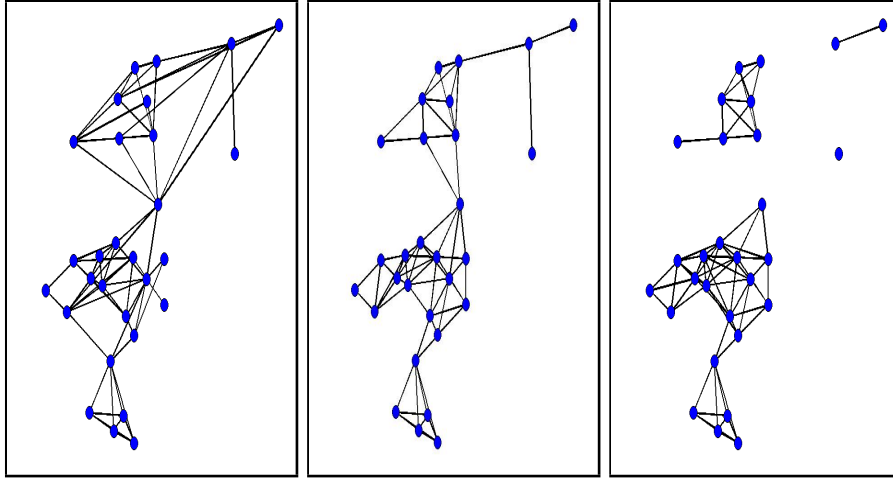$$ACC = \frac{TP + TN}{FP + FN + TP + TN}. \tag{5}$$

FIGURE 3. Comparison of rivalry networks. Each node in the network represents a gang's set space. An edge in the graph exists if there is a rivalry between the two gangs. The observed network (Left) is plotted with both the SBLN network from [22] (Middle) and the ecological territorial model from this paper (Right).

This value should fall between 0 and 1, with higher values indicating a more accurate graph. These values are presented in Table 2.

	TP	TN	FP	FN	ACC
Hegemann et al. SBLN	50	320	17	19	0.9113
Ecological Territorial Model	45	313	24	24	0.8818

TABLE 2. Accuracy measures for the Hegemann et al. SBLN model and the ecological territorial model.

While these accuracy measures are important, we would also like our rivalry network to have similar graph properties as the observed network. For example, the number of rivals that a gang has should be approximately the same in the simulation. Thus, we investigate features of the network related to the degree of a node $d(i)$, representing the number of rivals of a gang i. Three measures we use are the *graph density*, *degree variance*, and *Freeman's centrality measure*. Given G gangs, these are defined in [16, 48] as

$$\text{Density} = \frac{1}{G(G-1)} \sum_{i=1}^{G} d(i),$$

$$\text{Degree Variance} = \frac{1}{G} \sum_{i=1}^{G} \left[d(i) - \left(\frac{1}{G} \sum_{j=1}^{G} d(j) \right) \right]^2,$$

$$\text{Centrality} = \frac{1}{(G-1)(G-2)} \sum_{i=1}^{G} \left[\left(\max_{j} d(j) \right) - d(i) \right].$$

The density of the graph is a scalar multiple of the average degree. Thus, if two graphs have the same number of edges, then they will have the same density. The degree variance provides information on the spread of the degrees. Thus, a larger degree variance indicates a wider range of degrees, which translates to a larger spread in the number of rivals of each gang. The centrality measures whether there are key gangs that are more connected than the rest, indicating they are more central to the network. If all gangs have the same degree, i.e. no gang is more influential to the network, then the centrality measure would be zero. Alternatively, if one gang is connected to every other gang, and these are the only edges in the graph, then the network would have a high centrality measure.

These graph shape measures for the observed network, the Hegemann et al. SBLN network, and the ecological territorial model network are shown in Table 3. We note that the three networks have close values for the three metrics.

	Density	Degree Variance	Centrality
Observed Network	0.16995	4.32105	0.20106
Hegemann et al. SBLN	0.16503	3.54578	0.16799
Ecological Territorial Model	0.16995	5.70036	0.16270

TABLE 3. Graph metrics comparing the observed network with the Hegemann et al. SBLN model and the ecological territorial model.

While it is of interest to compare the rivalry network from the ecological territorial model to the observed network and the ones existing in the literature, we must also recognize that the method for obtaining the rivalry network from overlapping densities has limitations. More specifically, the edges that cross boundaries in the upper portion of the region are absent. This is expected since the model limits the smoothing of the gang densities across these boundaries. Thus, we do not anticipate much overlap in the territories of gangs in separate regions. Hence, we should examine other features of the model to determine the effectiveness of the model.

6.2. **Marking and gang densities.** Modeled gang and marking densities display some promising features. First, the gang densities $u^{(i)}$ remain centrally located about the known set spaces, with minimal overlap between gangs. Geographic boundaries limit the spread of gang density. Marking densities are highest between adjacent gangs that have a relatively small distance between them. Otherwise, the marking densities mimic the gang densities. This is expected as the steady-state solution of Equation (2) is given by

$$p^{(i)} = u^{(i)} \left[1 + m \sum_{j \neq i}^{n} p^{(j)} \right] \tag{6}$$

The plots of all gang and marking densities are provided together in Figure 4.

To better demonstrate the impact of the semi-permeable boundaries that represent the major roads and the river, the gang density for a central gang is shown in Figure 5. The set space for this particular gang is situated between two major freeways. To illustrate the impact of the southern boundary, we view the density
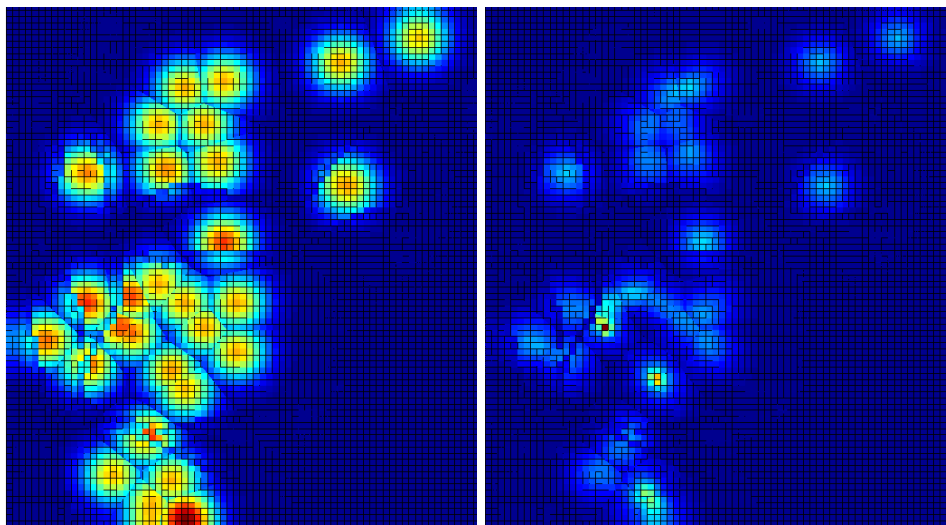
FIGURE 4. Simulated gang (Left) and marking (Right) densities in Hollenbeck. The densities for all of the gangs are plotted together. Red indicates a higher density and blue a lower density. The gang densities demonstrate the formation of territories and the impact of boundaries within the region. The marking densities are the highest between two close set spaces. Otherwise, the marking densities are similar to the gang densities.

facing East. Notice the dramatic drop in density over the boundary. Additionally, we see that some density still flows beyond the freeway as expected, since movement is not prohibited across boundaries, only discouraged.
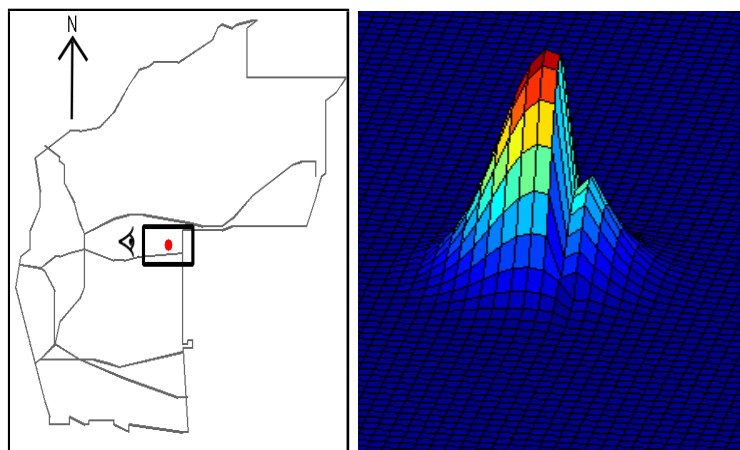
FIGURE 5. Impact of boundary on gang densities. The left figure shows the location of the set space for the gang of interest, represented by the dot situated between major roads. The eye symbol (Left) shows the lateral view for this gang's approximated density (Right). To demonstrate the impact of the southern boundary, the density is viewed facing East.

6.3. **Territories.** The ability to approximate gang territories is a desirable feature of this model. To do this, we classify a point (x, y) in space as belonging to the territory of gang i if

$$u^{(i)}(x, y) > u^{(j)}(x, y) \qquad \text{for all } j \neq i$$
$$u^{(i)}(x, y) > \delta.$$

Using this thresholding with δ, we limit the size of the territories so they do not cover the entire region. We took $\delta = 0.001$. The case where $\delta = 0$ is discussed in Section 6.4. The resulting territories are shown together in Figure 6. Although

FIGURE 6. Estimated gang territories. The semi-permeable boundaries of the model and the county line are plotted over the territories in white.

the semi-permeable boundaries highly influence the gang densities, some territory plots seem to extend beyond these boundaries. This is particularly evident for the southern boundary of the gang plotted in Figure 5.

6.4. **Voronoi diagrams.** Given a set of points, a Voronoi diagram partitions the area of interest into smaller regions that each contain only one of the points [15]. For a point x_A, we consider every pair (x_A, x_B) where $A \neq B$. We then construct a line between them that is equidistant to both points. After completing this for each point x_B, we take the resulting polygon that contains x_A. This is repeated for all points, decomposing the space into smaller regions. We compare the Voronoi diagram obtained from using the set spaces to the territories constructed with the ecological territorial model. We obtain interesting results if we consider $\delta = 0$ instead of $\delta = 0.001$ (i.e. no thresholding of the densities). Figure 7 overlays the partitioning line segments of the Voronoi diagram on the constructed territories with no thresholding. We notice that they align almost exactly.

For comparison, we do a simple approximation to the gang densities by using a Gaussian distribution centered at the set space. We used the parameter $\sigma = 3$ for the standard deviation of the distribution. Using the same technique for determining territories as above, we created a territory plot with no thresholding and plotted the Voronoi diagram over it as well. This is also shown in Figure 7. The boundaries of the territories match up exactly with the Voronoi diagram.
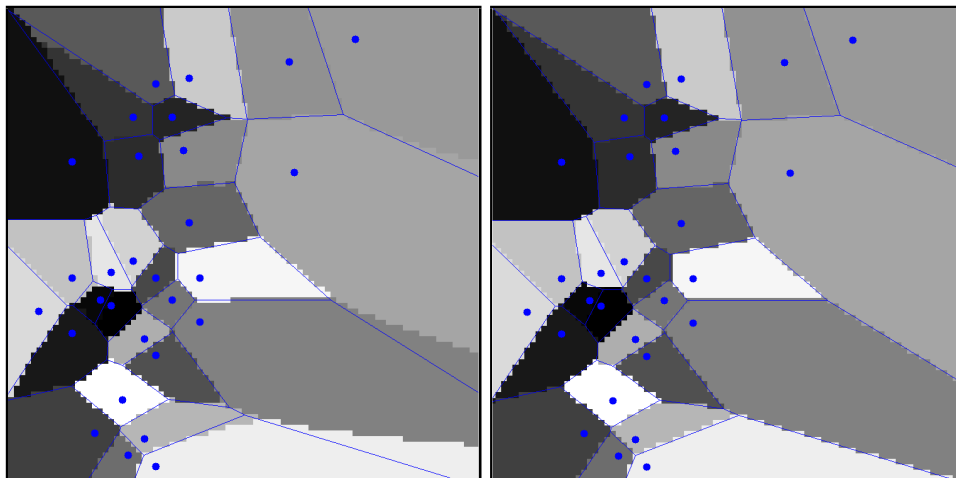
FIGURE 7. Voronoi plots compared to simulated territories. In both images, the set spaces for the gangs are represented by the solid circle. The solid lines give the Voronoi diagram for the region with input of the set spaces. The shaded regions provide the estimated gang territories with a Gaussian distribution for the gang densities (Right) and the $u^{(k)}$ gang densities obtained from the ecological territorial model (Left). Notice that the Gaussian distribution territories line up directly with the Voronoi plot, and the ecological territorial model only differs significantly on the far right portion of the region.

Both territory plots of Figure 7 and the Voronoi diagram produce a similar partitioning of the region. This suggests that the territories created using the ecological territorial model produces territories similar to using a standard normal distribution about the set space. However, we note that the normal distributions of separate gangs has significantly more overlap than the ecological territorial model gang densities. This does not show in these images as we only indicate which gang has a higher density here.

6.5. **Comparison of model densities with data.** As discussed in Section 5, we have two data sets with which we will compare our model output. The FI data provides the locations of where individuals have been stopped by the police. We assume this to be a reasonable sample of the gang densities. Thus, we plot the FI data over the gang densities in Figure 8. Additionally, we have violence data for interactions between gangs. These events are most likely to occur in locations where the marking density is high. Therefore, we plot this data over the marking densities in Figure 8.

To see how well the model fits the data, we examine the Akaike information criterion (AIC), given by

$$AIC = 2k - 2\ln(L), \tag{7}$$

where L is the likelihood function and k is the number of model parameters. The results are given in Table 4. In addition to the AIC values for the ecological territorial model, we examine the Gaussian distribution model. We find that the ecological territorial model performs better than the Gaussian distribution model when $\sigma = 3$, the standard deviation used in Figure 7. We optimized the σ to give the best AIC
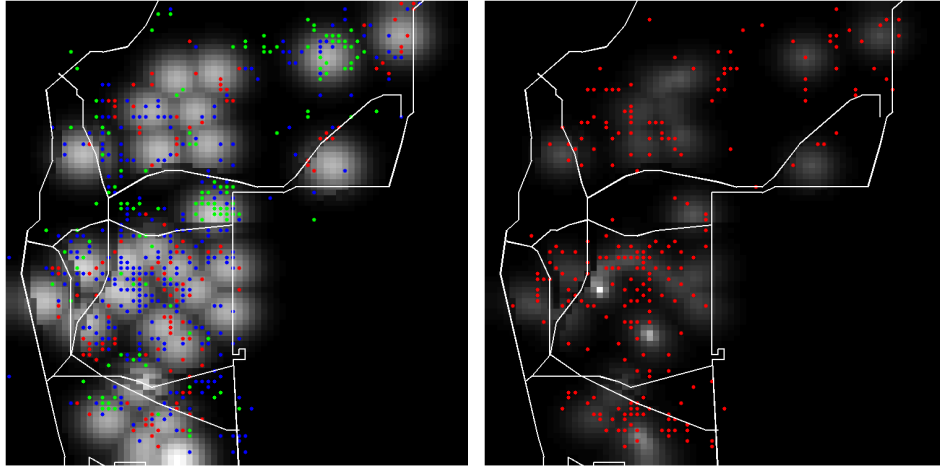
FIGURE 8. Data points and the simulated densities. The gang densities and the Field Interview data are plotted together (Left), and the marking densities are given with the violence data (Right). Here, the densities are provided as the background gray-scale image with whiter colors representing higher values. In the Field Interview data image (Left), the green dots are for individuals in their own theoretical territory, the red dots are for individuals in their rival gang's theoretical territory, and the blue dots are for the other cases.

measure, resulting in a value of $\sigma = 11.5$. However, theoretical territory plots for this value resulted in gangs having set spaces in other gangs' theoretical territories. This is an undesirable property, which is why the image is not included in the paper, but we include the AIC value in the table for comparison.

Method	Data Set	AIC
Ecological Territorial Model	FI Data	31150
Gaussian Distribution Model ($\sigma = 3$)	FI Data	41512
Gaussian Distribution Model ($\sigma = 11.5$)	FI Data	18207
Ecological Territorial Model	Violence Data	10526

TABLE 4. Akaike information criterion values for the ecological territorial model and the Gaussian distribution model. For the Gaussian distributions, we use $\sigma = 3$ as in Section 6.4 and $\sigma = 11.5$. The latter value gives the best AIC value, but creates territories that does not contain the set spaces for some gangs. Lower AIC values are desired.

Overall, we notice some interesting properties of the locations of the individuals in the FI data. Figure 8 plotted these data in different colors to correspond to the various cases. In particular, green dots represent gang members that are located in their own theoretical territory as estimated in Figure 6. The red dots show gang members located in a rival gang's theoretical territory, and the blue dots represent individuals that are neither in their own territory nor a rival gang's territory. Here, we determine a rival gang from the observed rivalry network. To help examine the individual cases, we plot them separately in Figure 9. We notice that the data
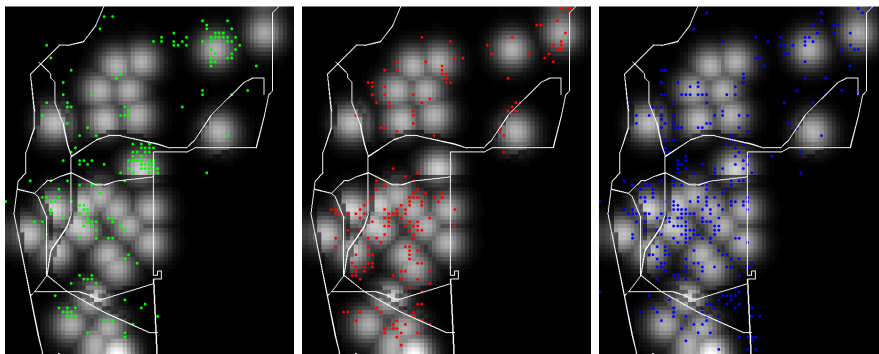
FIGURE 9. Field Interview data plotted over the gang densities determined by the ecological territorial model. The gang members in their own theoretical territories (Left), the gang members in their rival's theoretical territory (Middle), and the other cases (Right) are plotted here. A dot represents a location where a gang member was found. The gray-scale image in the background shows the gang densities estimated by the ecological territorial model.

points corresponding to locations where the gang members are not in their own theoretical territory are more likely to occur in areas near the boundaries of other gangs' theoretical territories. Perhaps these individuals were passing through the region by slipping between territories.

We highlight the FI data for three individual gangs in Figure 10. We notice that the densities visually indicate where to find the majority of the gang members. Instances where the individuals are not in the general vicinity of the home territory often occur near the major roads.
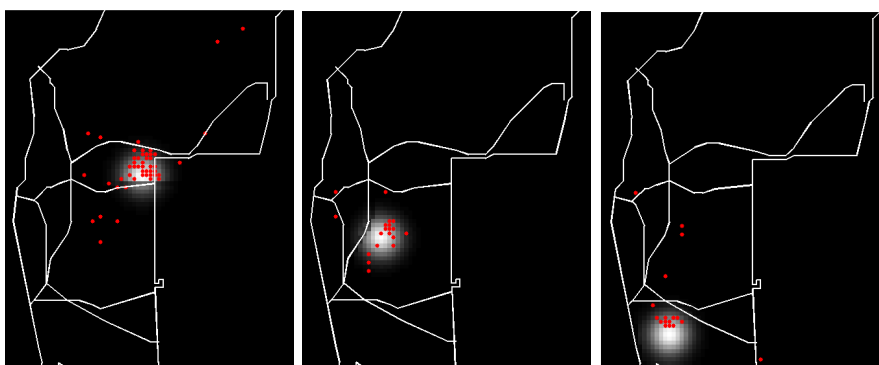

FIGURE 10. Field Interview data for three individual gangs. The red dots indicate the position of where a gang member was located. The gray-scale image provides the gang's density information estimated by the ecological territorial model.

Next, we examine the violence data and how it compares to the theoretical marking densities produced by the model. Table 4 provides the AIC value for the

violence data. Since we do not have another model to compare this with, we instead flag a certain portion of the city and find how many events occurred in this region. More specifically, we take all points such that for any i,

$$p^{(i)}(x,y) > \gamma \cdot \max_{j,x,y} \left(p^{(j)}(x,y) \right). \tag{8}$$

We took γ to be $0.2, 0.1$, and 0.05. The flagged regions are shown in Figure 11, and more information on the results are provided in Table 5. By flagging less than 14% of the cells, we predict more than half of the data.
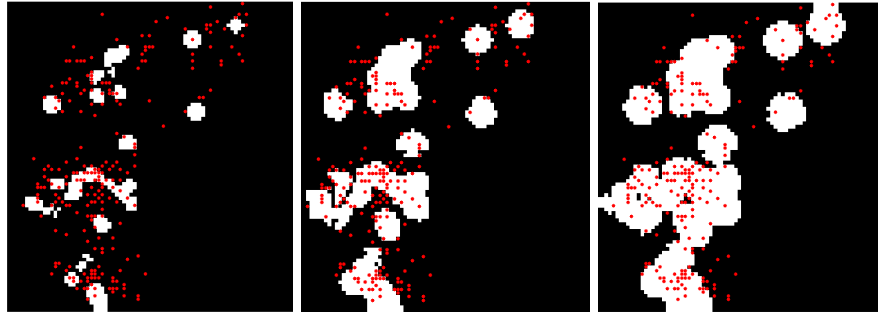

FIGURE 11. Violence data compared to flagged regions of the city. From left to right, we have $\gamma = 0.2, 0.1, 0.05$. The red dots indicate locations of violence between two gangs. The white regions are the flagged cells of the marking densities where we expect the events are more likely to occur.

γ	Percent of City Flagged	Percent of Violence Data Predicted
0.2	5.02%	20.61%
0.1	13.94%	50.91%
0.05	22.46%	71.21%

TABLE 5. Proportion of data predicted given a flagged region of the city.

6.6. **Rival gang territories and events.** Given approximate territories for gangs, we can investigate the locations of events with respect to these regions. Figure 12 gives the theoretical territories of three sets of rival gangs and the locations of the known violent interactions between them. Since we have information about which gang is the suspect and which is the victim, we illustrate which gang is the victim by matching the interior color of the marker with the territory color. In these three rivalries, we notice that all events occur near the boundaries of the theoretical territories. Events slightly to the interior of the theoretical territory boundary correspond with victim gangs in their own territory.

Sometimes there exists a rivalry between gangs of varying sizes. One such pair is illustrated in Figure 13, with one gang significantly larger than the other. Counterintuitively, the gang with the black set space is the larger gang and has a much greater number of events where it is the victim. We also notice that the smaller gang is only the victim on the boundary of the larger gang's theoretical territory or on the interior of its own theoretical territory. Since this data was recorded,
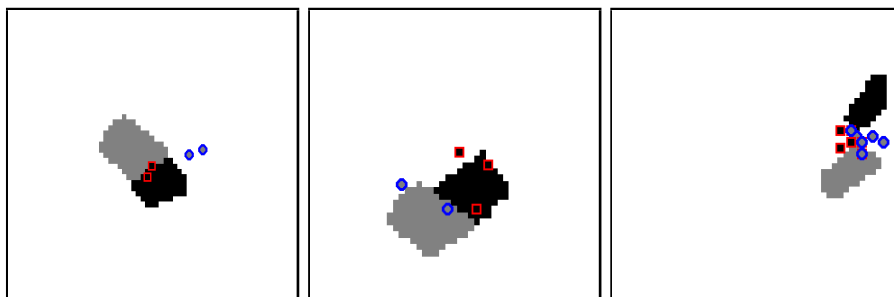
FIGURE 12. Territories and events of rival gangs. The three plots represent three pairs of rival gangs and the violent interactions between them. The interior color of the markers (circles and squares) indicates which gang is the victim by matching the color of its theoretical territory. All events occur near the boundaries of the territories.

the smaller gang collapsed after a key gang member was killed. Thus, the smaller number of attacks by the larger gang may have had more impact than the larger number made by the smaller gang.
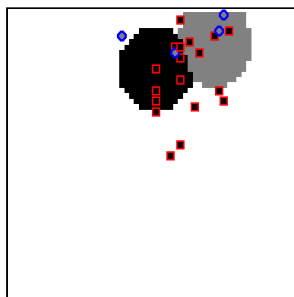

FIGURE 13. A rival pair of gangs with different sizes. The larger gang, whose theoretical territory is in black, is significantly larger than the smaller gang. The smaller gang is only the victim on the boundary of the larger gang's territory or on the interior of its own territory.

6.7. **Suspect versus victim.** In the previous section, we noticed a pattern where the locations of events occur with respect to theoretical territory boundaries. Figure 14 shows six pairs of rival gangs and where their violent interactions occurred. We notice a trend where the events typically fall either near the boundary of the approximated territories of either gang, on the interior of the victim's territory, or are far from either theoretical territory.

With this observation, we consider the location of events with respect to the boundaries of the approximate territories for both the suspect and the victim gangs. Previously, the authors of [8] investigated the positioning of the events with respect to a boundary line between gangs, equidistant to both set spaces. With the theoretical boundaries from the ecological territorial model, we are able to further analyze this data with respect to all boundaries. Given the victim gang's theoretical territory, we find the distance from an event to the territory boundary. We let this value be negative if the event occurs in the victim's territory and positive if it is outside.
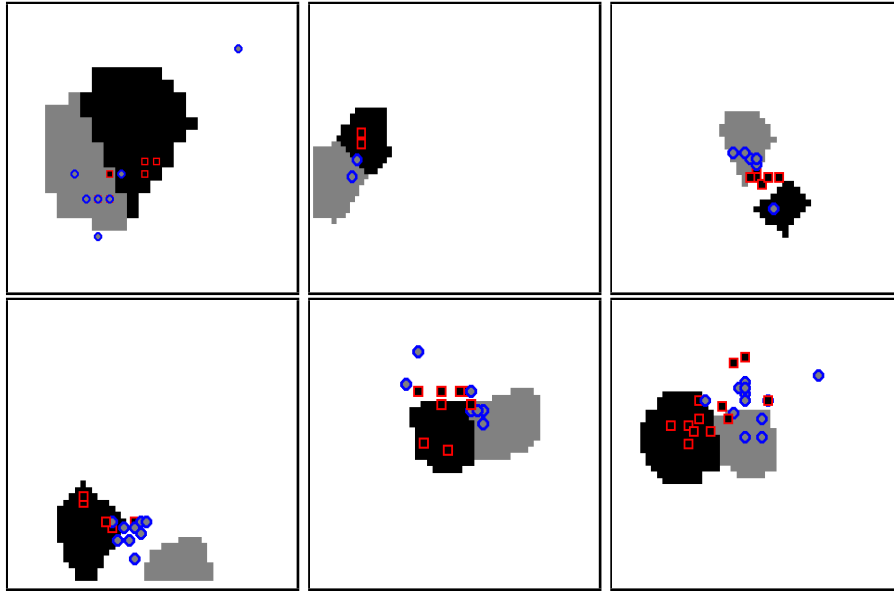
FIGURE 14. Rival gang territories and the events between them. The victim's gang's theoretical territory color matches the interior of the marker. The majority of events occur near the approximate territory boundaries, on the interior of the victim's territory, or away from both territories.

A histogram of these distances is provided in Figure 15, where one unit is equivalent to 0.1 km. We see that the events strongly cluster near the boundary of the victim.
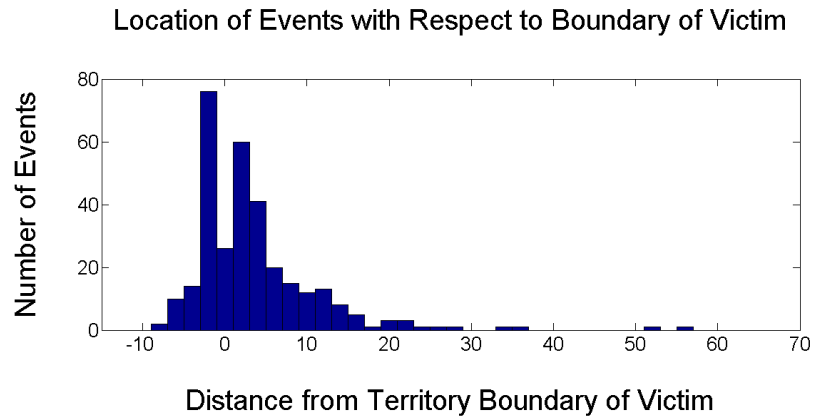

FIGURE 15. Histogram of the distance of an event to the boundary of the victim's theoretical territory. Negative values indicate the event occurred on the interior of the victim's territory, and positive values are for events on the exterior of the region. The distance is the number of grid units to the closest boundary point. 1 unit = 0.1 km.

We also note that the distribution is slightly skewed to have a larger number of events just interior to the victim's territory. This agrees with our observation in Figure 14.

Since the rival gangs are not necessarily adjacent to each other, we also repeat this analysis for the location of events with respect to the suspect's theoretical territory. Again, negative values indicate the event occurs on the interior of the suspect's territory, and positive values for the outside. The histogram is included in Figure 16. From this figure, we observe that the majority of events occur near
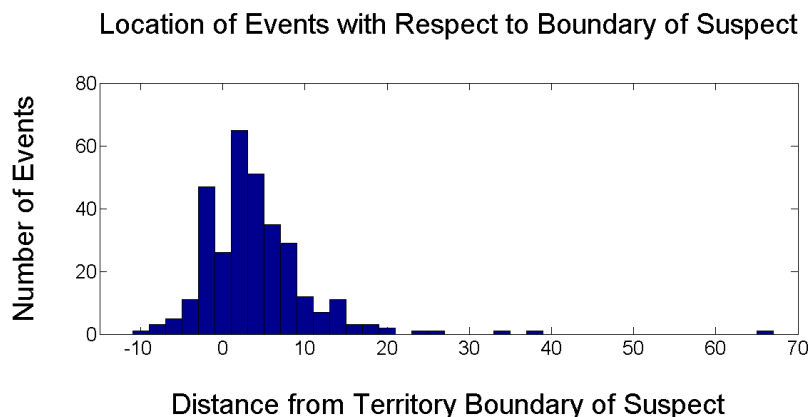

FIGURE 16. Histogram of the distance of an event to the boundary of the suspect's theoretical territory. Negative values indicate the event occurred on the interior of the suspect's territory, and positive values are for events on the exterior of the region. The distance is the number of grid units to the closest boundary point. 1 unit = 0.1 km.

the boundary of the suspect's territory, but skewed to the exterior of the region.

Quantitatively, we find 24.7% of the events occur within three grid units of the theoretical boundaries of both suspect and victim gangs. Additionally, 66.8% of the events occur within three grid units of either the suspect or victim gang's territory boundary.

7. **Discussion.** Using the framework of the coyote model proposed in [33], we formulated a model for street gang spatial behavior. This model was able to incorporate spatial features of the region that limit the movement individuals across these semi-permeable boundaries. For each gang, the model produced a gang density and marking density, indicating where gang members are expected to be and where their tags are most likely to be found.

As a first approach to evaluating our model, we compared the rivalry network from our model to the observed network and the Hegemann et al. SBLN network. While our model's network gave similar metric values, it did not outperform the SBLN network. This is due to the fact that we constructed the rivalry network from overlapping gang densities, which are discouraged from spreading beyond the semi-permeable boundaries encoded in the model. Thus, rivalries that cross these boundaries are not likely to be captured by the method we used to produce a

network. However, this method is able to provide more information than just a rivalry network. In particular, it can be used to approximate gang territories and the locations of violent interactions.

From the gang densities produced by the model, we approximated gang territories by classifying a point based on which gang has the highest density at that location. Without any thresholding, the resulting territory plot closely approximates a Voronoi diagram. With thresholding, the resulting territory plots give reasonable estimates for each gang's turf.

By flagging the cells with the highest theoretical marking densities, we were able to identify the majority of the violent events with a small portion of the city. Additionally, we were able to identify interesting behaviors of rival gangs. Events were more likely to occur in the interior of the victim gang's theoretical territory or on the boundary of either the victim or suspect gang's theoretical territory.

While comparing the gang densities to the FI data, we found the gang members were often not in the general vicinity of their approximated home territory. These individuals were frequently traveling on the boundaries of other gang's territories. Despite this, we demonstrated with three gangs that we were still able to give a good density estimate to the location of gang members.

As a next step in this modeling approach, we would like to include the gang sizes in the model. We would expect gangs with more individuals to produce more taggings and require more space. Additionally, we would like to incorporate other features that might impact the territory locations, such as police stations or multiple set spaces.

REFERENCES

[1] A. S. Ackleh, B. G. Fitzpatrick, R. Scribner, N. Simonsen and J. J. Thibodeaux, *Ecosystem modeling of college drinking: Parameter estimation and comparing models to data*, Mathematical and Computer Modelling, **50** (2009), 481–497.

[2] A. Alonso, "Urban Graffiti on the City Landscape," Western Geography Graduate Conference, San Diego State University, February 14, 1998.

[3] Elijah Anderson, "Code of the Street: Decency, Violence, and the Moral Life of the Inner City," W. W. Norton & Company, Inc., New York, 2000.

[4] J. Austin, E. Smith, S. Srinivasan and F. Sanchez, "Social Dynamics of Gang Involvement: A Mathematical Approach," Mathematical and Theoretical Biology Institute, MTBI-08-08M, 2011.

[5] A. Barbaro, L. Chayes and M. R. D'Orsogna, *Territorial development based on graffiti: A statistical mechanics approach*, 2011. Available from: ftp://ftp.math.ucla.edu/pub/camreport/cam11-70.pdf.

[6] Jordi Bascompte and Ricard V. Sole, *On wolf territoriality and deer survival*, in "Modeling Spatiotemporal Dynamics in Ecology," Springer-Verlag, New York, (1998), 105–126.

[7] L. M. A. Bettencourt, A. Cintròn-Arias, D. I. Kaiser and C. Castillo-Chàvez, *The power of a good idea: Quantitative modeling of the spread of ideas from epidemiological models*, Physica A: Statistical Mechanics and its Applications, **364** (2006), 513–536.

[8] P. J. Brantingham, G. Tita, M. B. Short and S. Reid, *The ecology of gang territorial boundaries*, Criminology, in press.

[9] B. Briscoe, M. Lewis and S. Parrish, *Home range formation in wolves due to scent marking*, Bulletin of Mathematical Biology, **64** (2002), 261–284.

[10] W. K. Brown, *Graffiti, identity and the delinquent gang*, Internal Journal of Offender and Comparative Criminology, **22** (1978), 46–48.

[11] S. H. Decker and B. Van Winkle, "Life in the Gang: Family, Friends, and Violence," Cambridge University Press, New York, New York, 1996.

[12] Perri K. Eason, Gary A. Cobbs and Kristin G. Trinca, *The use of landmarks to define territorial boundaries*, Animal Behavior, **58** (1999), 85–91.

[13] J. Eck and L. Liu, *Contrasting simulated and empirical experiments in crime prevention*, Journal of Experimental Criminology, 2008.

[14] Mike Egesdal, Chris Fathauer, Kym Louie and Jeremy Neuman, *Statistical modeling of gang violence in Los Angeles*, SIAM Undergraduate Research Online, **3** (2010).

[15] S. Fortune, *Voronoǐ diagrams and Delaunay triangulations*, in "Computing in Euclidean Geometry" (eds. D. Du and F. Hwang), Lecture Notes Ser. Comput., **1**, World Scientific Publ., River Edge, NJ, (1992), 193–233.

[16] Linton C. Freeman, *Centrality in social networks conceptual clarification*, Social Networks, **1** (1979), 215–239.

[17] Celeste Fremon, "G-Dog and the Homeboys: Father Greg Boyle and the Gangs of East Los Angeles," University of New Mexico Press, Albuquerque, New Mexico, 2008.

[18] Luca Giuggioli, Jonathan R. Potts, and Stephen Harris, *Animal interactions and the emergence of territoriality*, PLoS Computational Biology, **7** (2011), 1–9.

[19] Mirta B. Gordon, *A random walk in the literature on criminality: A partial and critical view on some statistical analyses and modelling approaches*, European Journal of Applied Mathematics, **21** (2010), 283–306.

[20] Kristen Hawkes, Kim Hill and James F. O'Connell, *Why hunters gather: Optimal foraging and the Achè of eastern Paraguay*, American Ethnologist, **9** (1982), 379–398.

[21] Rachel A. Hegemann, Erik A. Lewis and Andrea L. Bertozzi, *An "Estimate & Score Algorithm" for simultaneous parameter estimation and reconstruction of missing data on social networks*, 2012. Available from: `ftp://ftp.math.ucla.edu/pub/camreport/cam12-12.pdf`.

[22] Rachel A. Hegemann, Laura M. Smith, Alethea B. T. Barbaro, Andrea L. Bertozzi, Shannon E. Reid and George E. Tita, *Geographical influences of an emerging network of gang rivalries*, Physica A: Statistical Mechanics and its Applications, **390** (2011), 3894–3914.

[23] E. E. Holmes, M. A. Lewis, J. E. Banks and R. R. Veit, *Partial differential equations in ecology: Spatial interactions and population dynamics*, Ecology, **75** (1994), 17–29.

[24] S. R. Jammalamadaka and A. SenGupta, "Topics in Circular Statistics," Series on Multivariate Analysis, **5**, World Scientific Publishing Co., Inc., River Edge, NJ, 2001.

[25] Jill E. Jankowski, Scott K. Robinson and Douglas J. Levey, *Squeezed at the top: Interspecific aggression may constrain elevational ranges in tropical birds*, Ecology, **91** (2010), 1877–1884.

[26] Matthew James Keeling and Pejman Rohani, "Modeling Infectious Diseases in Humans and Animals," Princeton University Press, Princeton, New Jersey, 2008.

[27] Malcolm Klein and Cheryl Maxson, "Street Gang Patterns and Policies," Oxford University Press, Oxford, New York, 2006.

[28] M. A. Lewis and J. D. Murray, *Modelling territoriality and wolf-deer interactions*, Nature, **366** (1993), 738–740.

[29] M. A. Lewis, K. A. White and J. D. Murray, *Analysis of a model for wolf territories*, Journal of Mathematical Biology, **35** (1997), 749–774.

[30] David Ley and Roman Cybriwsky, *Urban graffiti as territorial markers*, Annals of the Association of American Geographers, **64** (1974), 491–505.

[31] Paul R. Moorcroft and Alex Barnett, *Mechanistic home range models and resource selection analysis: A reconciliation and unification*, Ecology, **89** (2008), 1112–1119.

[32] Paul R. Moorcroft, Mark A. Lewis and Robert L. Crabtree, *Home range analysis using a mechanistic home range model*, Ecology, **80** (1999), 1656–1665.

[33] Paul R. Moorcroft, Mark A. Lewis and Robert L. Crabtree, *Mechanistic home range models capture spatial patterns and dynamics of coyote territories in Yellowstone*, Proceedings: Biological Sciences, The Royal Society, **273** (2006), 1651–1659.

[34] Joan Moore, "Homeboys: Gangs, Drugs, and Prison in the Barrios of Los Angeles," Temple University Press, Philadelphia, 1978.

[35] Joan Moore, "Going Down to the Barrio: Homeboys and Homegirls in Change," Temple University Press, Philadelphia, 1991.

[36] Joan Moore, Diego Vigil and Robert Garcia, *Residence and Territoriality in Chicano Gangs*, Social Problems, **31** (1983), 182–194.

[37] Roger P. Peters and L. David Mech, *Scent-marking in wolves: Radio-tracking of wolf packs has provided definite evidence that olfactory sign is used for territory maintenance and may serve for other forms of communication within the pack as well*, American Scientist, **63** (1975), 628–637.

[38] S. Radil, C. Flint and G. Tita, *Spatializing social networks: Using social network analysis to investigate geographies of gang rivalry, territoriality, and violence in Los Angeles*, Annals of the Association of American Geographers, **100** (2010), 307–326.

[39] D. M. Romero, C. M. Kribs-Zaleta, A. Mubayi and C. Orbe, *An epidemiological approach to the spread of political third parties*, Social Sciences Research Network, 2009. Available from: http://dx.doi.org/10.2139/ssrn.1503124.

[40] Pamela Effrein Sandstrom, *An optimal foraging approach to information seeking and use*, The Library Quarterly, **64** (1994), 414–449.

[41] M. Short, G. Mohler, P. J. Brantingham and G. Tita, *Gang rivalry dynamics via coupled point process networks*, 2011. Available from: http://math.scu.edu/~gmohler/gangnetwork.pdf.

[42] A. Stomakhin, M. B. Short and A. L. Bertozzi, *Reconstruction of missing data in social networks based on temporal patterns of interactions*, Inverse Problems, **27** (2011), 115013, 15 pp.

[43] Travis A. Taniguchi, Jerry H. Ratcliffe and Ralph B. Taylor, *Gang set space, drug markets, and crime around drug corners in Camden*, Journal of Research in Crime and Delinquency, **48** (2011), 327–363.

[44] F. M. Thrasher, "The Gang: A Study of 1313 Gangs in Chicago," University of Chicago Press, Chicago, 1927.

[45] G. Tita, J. Cohen and J. Engberg, *An ecological study of the location of gang "set space"*, Social Problems, **52** (2005), 272–299.

[46] G. Tita, K. Riley, G. Ridgeway, C. Grammich, A. Abrahamse and P. Greenwood, "Reducing Gun Violence: Results from an Intervention in East Los Angeles," RAND Corporation, Santa Monica, California, 2003.

[47] James Vigil, "Barrio Gangs: Street Life and Identity in Southern California," University of Texas Press, Austin, Texas, 1988.

[48] Stanley Wasserman and Katherine Faust, "Social Network Analysis: Methods and Applications," Cambridge University Press, New York, 2009.

[49] David P. Watts and John C. Mitani, *Boundary patrols and intergroup encounters in wild chimpanzees*, Behaviour, **138** (2001), 299–327.

[50] K. A. White, M. A. Lewis and J. D. Murray, *A model for wolf-pack territory formation and maintenance*, Journal of Theoretical Biology, **178** (1996), 29–43.

E-mail address: lsmith@math.ucla.edu
E-mail address: bertozzi@math.ucla.edu
E-mail address: pjb@anthro.ucla.edu
E-mail address: gtita@uci.edu
E-mail address: mvalasik@uci.edu